

Folding of the Yeast Prion Protein Ure2: Kinetic Evidence for Folding and Unfolding Intermediates

Despina Galani¹, Alan R. Fersht¹ and Sarah Perrett^{1,2*}

¹Centre for Protein Engineering, Department of Chemistry, University of Cambridge, Lensfield Road Cambridge, CB2 1EW, UK

²National Laboratory of Biomacromolecules, Institute of Biophysics, Chinese Academy of Sciences, 15 Datun Road Chaoyang District, Beijing 100101, China

The *Saccharomyces cerevisiae* non-Mendelian factor [URE3] propagates by a prion-like mechanism, involving aggregation of the chromosomally encoded protein Ure2. The N-terminal prion domain (PrD) of Ure2 is required for prion activity *in vivo* and amyloid formation *in vitro*. However, the molecular mechanism of the prion-like activity remains obscure. Here we measure the kinetics of folding of Ure2 and two N-terminal variants that lack all or part of the PrD. The kinetic folding behaviour of the three proteins is identical, indicating that the PrD does not change the stability, rates of folding or folding pathway of Ure2. Both unfolding and refolding kinetics are multiphasic. An intermediate is populated during unfolding at high denaturant concentrations resulting in the appearance of an unfolding burst phase and “roll-over” in the denaturant dependence of the unfolding rate constants. During refolding the appearance of a burst phase indicates formation of an intermediate during the dead-time of stopped-flow mixing. A further fast phase shows second-order kinetics, indicating formation of a dimeric intermediate. Regain of native-like fluorescence displays a distinct lag due to population of this on-pathway dimeric intermediate. Double-jump experiments indicate that isomerisation of Pro166, which is *cis* in the native state, occurs late in refolding after regain of native-like fluorescence. During protein refolding there is kinetic partitioning between productive folding *via* the dimeric intermediate and a non-productive side reaction *via* an aggregation prone monomeric intermediate. In the light of this and other studies, schemes for folding, aggregation and prion formation are proposed.

© 2002 Academic Press

Keywords: Ure2p; off-pathway; lag phase; protein folding; protein folding pathway

*Corresponding author

Introduction

The concept of a prion presents a fascinating challenge to our understanding of the way proteins fold.¹ The discovery of prion-like proteins in bakers' yeast has facilitated research into this phenomenon.^{2,3} However, the actual mechanism by which an altered protein conformation might be propagated remains mysterious. The [URE3] non-Mendelian genetic element of *Saccharomyces cer-*

*visiae*⁴ propagates by a prion-like mechanism *via* transmission of an aggregated form of the chromosomally encoded protein Ure2.⁵ The prion phenotype corresponds to loss of the cellular function of Ure2, an enzyme involved in regulation of nitrogen metabolism. Ure2 is a dimer in solution^{6,7} and the peptide chain consists of two regions. The unstructured N-terminal region^{7,8} is rich in asparagine and glutamine and is required for the prion function *in vivo*⁹ and amyloid formation *in vitro*.^{6,10,11} The compactly folded C-terminal region,^{7,8} for which the crystal structure has been solved,^{12,13} conveys the enzymatic function⁹ and has homology to glutathione *S*-transferases.¹⁴ A first step in understanding the molecular mechanism by which the N-terminal prion domain (PrD) might exert its prion forming ability is to determine how the PrD affects the intrinsic properties of the Ure2 protein in isolation from cellular cofactors. We set out to address this question by constructing a series of

Present address: D. Galani, Harokopio University, 70 El. Venizelou Str., 176-71 Athens, Greece.

Abbreviations used: 90Ure2, Ure2 in which residues 1-89 have been deleted; Δ15-42Ure2, Ure2 in which residues 15-42 have been deleted; a.u., arbitrary units; CD, circular dichroism; GdmCl, guanidinium chloride; PrD, prion domain.

E-mail address of the corresponding author: sarah.perrett@iname.com

Ure2 variants that lack all or part of the PrD.⁷ We have previously shown that removal of all or part of the PrD does not affect the oligomeric state or thermodynamic stability of the protein.⁷ Ure2 has a propensity to misfold⁷ and aggregate,^{6–8,10,11} properties that are irrespective of the presence of the PrD.^{7,11} Here we use conditions optimised for reversibility of folding (25 °C and pH 8.4) to determine the effect of the PrD on the kinetic rates of folding and unfolding of Ure2. We compare three Ure2 variants: full-length Ure2; 90Ure2 which lacks the N-terminal glutamine/asparagine-rich PrD; and Δ 15-42Ure2, in which the 28 residue island of “normal” amino acid sequence within the PrD has been excised.⁷

The rates of folding and unfolding obtained for the three proteins were the same, indicating that the PrD does not affect the stability or rates of folding of Ure2. The kinetics of both unfolding and refolding of Ure2 were found to be complex. A reaction scheme for folding which accounts for the available data is proposed. A possible mechanism for Ure2 prion formation is also postulated, which accounts for the apparent contradiction between *in vivo* and *in vitro* experiments regarding interaction between the C-terminal region and the prion domain.¹³

Results

Unfolding kinetics

The kinetics of unfolding of full-length Ure2, 90Ure2 and Δ 15-42Ure2 was measured at GdmCl concentrations ranging from the mid-point of unfolding (3.0 M) to the limit before rates became too fast to be measured accurately in the stopped-flow apparatus (6.0 M).

Ure2 displays multiphasic unfolding kinetics

When unfolding in GdmCl concentrations around 4.0 M the data fit well to a single exponential equation (Figure 1(a)). Around 4.5 M GdmCl, the residual for fitting to a single exponential with linear drift is small (less than 0.2% of the total amplitude) but shows systematic variation which is removed by fitting to a double exponential (Figure 1(b)). Above 5.0 M GdmCl, the multiphasic nature of the traces apparently increases in complexity (Figure 1(c)). The rate constants obtained by fitting to a sum of two or more exponentials differ at most by a factor of three, so the phases cannot be clearly distinguished. The data were, therefore, fitted to a single exponential decay

† There is no *in vitro* enzymatic assay available for Ure2. The term “native” is used throughout to mean the never-unfolded, dimeric structure populated in the absence of any denaturant. As shown here, the “native” state can also be identified by its rate of unfolding, which is slower than for the kinetically more labile folding intermediates observed.

throughout. Incubation of the protein overnight in 1.5 M GdmCl before unfolding produced identical unfolding traces (Figure 1(a)) and observed rate constants (Figure 2(a)) to unfolding from 0 M GdmCl. This suggests that the multiphasic unfolding kinetics do not arise from heterogeneity in the native state.¹⁵

Non-linear denaturant dependence of unfolding rate constants

Figure 2(a) shows the denaturant dependence of the rate constants. The observed unfolding rate constants for the three proteins were fitted to a linear equation of the form:

$$\ln k_{\text{obs}} = \ln k_{\text{H}_2\text{O}} + m[\text{GdmCl}] \quad (1)$$

where $k_{\text{H}_2\text{O}}$ is the rate constant for unfolding in the absence of denaturant and m is the slope. The values obtained are shown in Table 1. Above 5.5 M GdmCl the data show deviation from linearity. This is not the smooth curvature that is attributed to the Hammond effect and that can be treated by fitting to a polynomial of the form:

$$\ln k_{\text{obs}} = \ln k_{\text{H}_2\text{O}} + m[\text{GdmCl}] + m^*[\text{GdmCl}]^2 \quad (2)$$

instead of a linear equation.^{16,17} The Ure2 unfolding data do not fit well to a second-order polynomial. The relatively abrupt deviation from linearity observed here is indicative of a change in mechanism or rate determining step. This suggests the population of an intermediate during unfolding at high denaturant concentrations.^{18,19}

A burst phase is observed in unfolding

The denaturant dependence of the folding amplitudes is shown in Figure 2(b) and (c). Between 3.0 and 5.0 M GdmCl, the unfolding amplitudes obtained are consistent with the equilibrium values;⁷ no burst phase is detected. Above 5.0 M GdmCl a “negative burst phase” is observed, that is to say, the initial fluorescence value is higher than expected for native† protein and the unfolding amplitudes show an increase (Figure 2(b)). The sigmoidal denaturant dependence of the amplitude of the burst phase is consistent with the population of an intermediate during unfolding which has fluorescence greater than the native state.¹⁹

In all cases the observed rate constants and their dependence on GdmCl concentration are the same within error for the three proteins (Figure 2(a) and Table 1). This indicates that the PrD does not affect the rate or pathway of unfolding of Ure2.

Refolding kinetics

In all cases the observed refolding behaviour was the same for Ure2, 90Ure2 and Δ 15-42Ure2 (Figure 2(a)), supporting the conclusion that deletion of the PrD does not affect the stability, folding kinetics or folding pathway of Ure2, nor does

Table 1. Unfolding rates in water and equilibrium values for Ure2, 90Ure2 and $\Delta 15-42$ Ure2

	Kinetic values ^a		Equilibrium values ^b	
	k_{u,H_2O} (s ⁻¹)	m_u (M ⁻¹)	$\Delta G_{D-N,H_2O}$ (kcal mol ⁻¹)	m_{eq} (kcal mol ⁻¹ M ⁻¹)
Ure2	5 (± 2) $\times 10^{-12}$	4.82 (± 0.07)	12.4 (± 0.5)	4.2 (± 0.2)
90Ure2	10 (± 3) $\times 10^{-12}$	4.70 (± 0.06)	11.2 (± 0.8)	3.8 (± 0.4)
$\Delta 15-42$ Ure2	7 (± 1) $\times 10^{-12}$	4.78 (± 0.04)	13.0 (± 1.2)	4.4 (± 0.4)
Combined data ^c	8 (± 1) $\times 10^{-12}$	4.74 (± 0.03)	12.4 (± 0.4)	4.2 (± 0.2)

The errors (the standard error from the fit, or of the mean, as appropriate) are shown in parentheses.

^a Obtained by fitting the data shown in Figure 2(a) to equation (1).

^b Equilibrium data taken from Perrett *et al.*⁷

^c The combined kinetic data were obtained by simultaneous fitting of the data for all three proteins. The combined equilibrium data represent mean values which include two other similar Ure2 constructs, 15Ure2 and 74Ure2.⁷

it remove the tendency to undergo aggregation during folding. The three proteins are therefore treated together.

Three refolding phases are observed: a burst phase that is complete within the dead-time of mixing in the stopped-flow apparatus (millisecond timescale), a fast phase (complete within seconds) and a slow phase (complete within minutes to hours). Between 1.0 and 2.0 M GdmCl, interpretable refolding data could not generally be obtained. Light scattering (not shown) and velocity sedimentation analytical ultracentrifugation (J.P.G. Butler & S.P., unpublished results) indicate the presence of aggregation in this region.

Detection of native or intermediate states is biased by the choice of emission wavelength(s)

Comparison of the refolding traces obtained in the stopped-flow apparatus using a 320 nm emission cut-off filter with those obtained in a stopped-flow apparatus equipped with a monochromator (set at 327 nm) suggests that monitoring at a single wavelength is more sensitive for detection of the native (or native-like) state, whereas the use of the cut-off filter is more sensitive for detection of one or more of the intermediates formed (see also Materials and Methods). In the experiments described here, the fast phase was measured in the stopped-flow apparatus using a 320 nm cut-off filter, whereas the slow phase was measured in a fluorimeter monitoring at a single emission wavelength of 327 nm. The relative amplitudes of the phases and the observed fluorescence relative to the fluorescence of the native state are therefore different in the two instruments. For this reason, the actual measured fluorescence values under the two experimental set-ups are shown separately (Figure 2(b) and (c)), without any attempt to normalise between the two.

The refolding kinetics shows a burst phase and a fast phase

The fast phase was measured between 0.5 and 1.0 M GdmCl. A significant proportion of the

native fluorescence signal is regained within the deadtime of stopped-flow mixing, i.e. there is a burst phase. This indicates the formation of an intermediate within milliseconds of initiation of refolding. Between 0.5 M and 1.0 M GdmCl the amplitude of the burst phase increases and the amplitude of the fast phase decreases (Figures 2(b) and 3(a)).

Concentration dependence of the fast phase indicates a dimeric intermediate

The fast phase can be fitted to a single exponential with linear drift. However, plotting the rate constants thus obtained against protein concentration (Figure 3(b)) reveals that the process is not in fact first-order, but shows protein concentration dependence. This indicates fitting to a second-order equation of the form:

$$S(t) = S(t_\infty) - (A/(P_T kt + 1)) \quad (3)$$

where $S(t)$ is the fluorescence signal at recorded time t , $S(t_\infty)$ is the endpoint, A is the amplitude, P_T is the total (monomeric) protein concentration and k is the rate constant.²⁰ The second-order rate constants obtained are the same within error at protein concentrations within the range 0.5-4 μ M. This rules out the possibility of higher-order stoichiometries and is consistent with the dimeric structure of the native state.

The GdmCl dependence of the second-order rate constants for formation of the dimeric intermediate are plotted in Figure 2(a) and the value of k_{H_2O} obtained by fitting the observed second-order rate constants to equation (1) is given in Table 2 (as k_{fast}).

Slow regain of native-like fluorescence

The slow phase was measured between 0.1 M and 2.5 M GdmCl by manual mixing in a fluorimeter, which allowed acquisition over longer times or at dilution ratios of greater than 1:10. This slow phase fits well to a single exponential equation (Figure 4(a) and (b)). No slower phases were observed in folding.

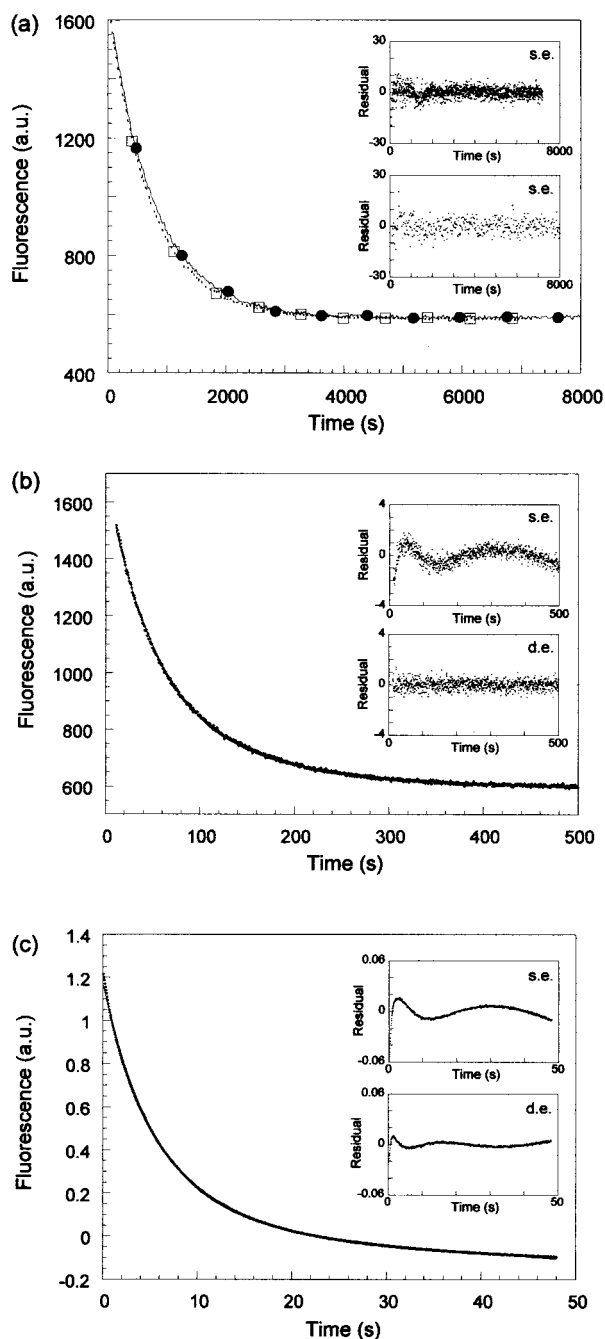


Figure 1. Typical kinetic traces for unfolding of 1 μM Ure2, 90Ure2 or $\Delta 1542\text{Ure2}$ in 50 mM Tris-HCl (pH 8.4) containing 200 mM NaCl at 25 $^{\circ}\text{C}$ monitored by fluorescence. The quality of the fit to a single (s.e.) or double (d.e.) exponential is indicated by the residual (insets). Fitting to a single exponential is shown ((b) and (c)). (a) Unfolding in a final GdmCl concentration of 4.0 M initiated from 0 M (\square ; upper inset panel) or 1.5 M GdmCl (\bullet ; lower inset panel). (b) Unfolding in 4.5 M GdmCl. (c) Unfolding in 5.0 M GdmCl.

The fast phase is generally complete within the dead-time of manual mixing and about 85% of the expected regain in fluorescence occurs within this

dead-time (when monitoring at 327 nm; Figure 2(c)). Around 0.6 M GdmCl, where no aggregation is detected (see Materials and Methods), the slow phase accounts for the remaining 15% of amplitude. However, at GdmCl concentrations approaching 1 M, the overall regain in fluorescence decreases (Figure 2(c)), indicating a decrease in refolding yield. This coincides with the region where the dimeric intermediate is no longer significantly populated and indicates the occurrence of a non-productive side-reaction. This is consistent with the observed occurrence of aggregation in this region and coincides with the hysteresis observed in the refolding reaction when equilibrium experiments are performed under non-reversible refolding conditions.⁷

The GdmCl dependence of the slow phase (Figure 2(a)) indicates that it represents folding and not an isomerisation or rearrangement event. The data measured between 0.5 M and 2.5 M GdmCl fit well to a linear equation. The value of $k_{\text{H}_2\text{O}}$ obtained by fitting the observed slow phase rate constants to equation (1) is given in Table 2 (as k_{slow}). Below 0.5 M GdmCl the observed rate constants show a plateau in the GdmCl dependence, behaviour that indicates either aggregation²¹ or the population of an intermediate during refolding at low denaturant concentrations.²² The latter is consistent with the observation of the fast phase due to formation of an intermediate at low denaturant concentrations. The value of $k_{\text{H}_2\text{O}}$ obtained by fitting the observed rate constants including the plateau region to a second-order polynomial (equation (2)) is given in Table 2 (as k_{plateau}).

The slow phase does not show any pronounced protein concentration dependence (Figure 4(c)). There is some indication of protein concentration dependence around the inflection point where the change in observed refolding mechanism occurs. This is consistent with stabilisation of the dimeric intermediate at higher protein concentrations, which then causes a decrease in the observed rate of folding.

Observation of a lag phase

The slow phase, when observed in the stopped-flow traces, shows a distinct lag, which increases with increasing GdmCl concentration and decreases with increasing protein concentration (Figure 5). At 1 μM protein concentration, where the lag is long, the curves measured between 0.5 M and 1.0 M GdmCl are best described by an equation of the form:

$$S(t) = S(t_{\infty}) + A_1 e^{(-k_1 t)} - (A_2 / (P_T k_2 t + 1)) \quad (4)$$

corresponding to the formation and disappearance of a dimeric intermediate (Figure 3(c)). The rate of the exponential decay is identical to the rate of slow regain of native fluorescence measured by manual mixing (monitored at 327 nm; Figures 2(a) and 4). At higher protein concentrations, the

Table 2. Combined data for the kinetics of refolding of Ure2, 90Ure2 and $\Delta 15-42$ Ure2

	k_{f,H_2O}	m_f (M ⁻¹)	m_f^* (M ⁻²)
k_{fast} (s ⁻¹ M ⁻¹)	$2.7 (\pm 0.8) \times 10^6$	$-3.03 (\pm 0.3)$	-
k_{slow} (s ⁻¹)	$0.20 (\pm 0.01)$	$-2.71 (\pm 0.05)$	-
$k_{plateau}$ (s ⁻¹)	$0.07 (\pm 0.02)$	$-0.9 (\pm 0.4)$	$-0.6 (\pm 0.2)$

The values shown were obtained by fitting of the data shown in Figure 2(a). k_{fast} was obtained by fitting the second-order rate constants for the fast phase of refolding to equation (1). k_{slow} was obtained by fitting the first-order rate constants for the slow phase of refolding in the linear region between 0.5 and 2.5 M GdmCl to equation (1). $k_{plateau}$ was obtained by fitting the same slow phase rate constants, but including the plateau region below 0.5 M GdmCl, to equation (2). The errors taken from the fits are shown in parentheses.

second-order fast phase, the exponential decay, the lag and the subsequent slow regain of native fluorescence are all apparent in the stopped-flow traces (Figure 5). The observation of a lag phase indicates that the dimeric intermediate is on-pathway and obligate to formation of the native state.

Double jump experiments

Half-lives for *cis-trans* isomerisation of proline bonds are typically of the order of 10-100 seconds. Ure2 has 12 proline residues, one of which is in a *cis* conformation in the native state, therefore proline limited phases could be expected to be significant. The ratio of *trans:cis* proline in an unstructured polypeptide is estimated to be at least 5:1.^{23,24} Based on this it can be estimated that around 2% (i.e. $(1/6) \times (5/6)^{11}$) of unfolded Ure2 molecules have all Pro residues in their native conformation, approximately 17% have Pro166 in a native *cis* conformation and approximately 83% have any other individual proline in a native *trans* conformation.

The effect on the folding pathway of a non-native proline bond is variable. In some proteins, folding cannot occur until isomerisation takes place.²⁵ In others, the protein can fold to an intermediate conformation,²⁶ or to a state that is native-like, with proline isomerisation occurring in a final, slow step.^{23,27-29} These alternatives can generally be distinguished by the application of double-jump stopped-flow methods.³⁰

Double-jump refolding

Double-jump refolding experiments can be used to test whether any of the phases observed in single-jump refolding experiments are linked to proline isomerisation events. Double-jump refolding performed under conditions limited for proline isomerisation (see Materials and Methods) gave monophasic traces with rate constants identical to those measured for the fast phase of refolding under single-jump conditions. The same decrease in amplitude with increasing GdmCl concentration was observed. This indicates that the observation of multiple kinetic phases for refolding is not the result of heterogeneity in the denatured state due to the presence of different *cis-trans* proline iso-

mers. This also demonstrates that folding to the dimeric intermediate formed during the fast phase is not limited by proline isomerisation.

Double-jump unfolding

Double-jump unfolding experiments can be used to distinguish between different native-like forms on the basis of their different rates of unfolding.³¹ To investigate whether refolding to the native state occurs on the same timescale as the slowest of the observed refolding phases, double-jump unfolding experiments were performed. Denatured protein was allowed to refold for varying times (one second to one hour) in 0.5 M GdmCl before unfolding again. The half-life for the slowest observed refolding phase under these conditions in single-jump experiments is approximately 14 seconds, so on the basis of the observable refolding phases, refolding is expected to be 95% complete within one minute. However, we found that on re-unfolding after delays of one minute to one hour, approximately 80% of the amplitude is lost in a rapid phase (complete within seconds). The subsequent traces were otherwise the same as for single-jump unfolding. This suggests that within the delay time only approximately 20% of molecules attain the native state, with the remainder of molecules in a conformation that is less stable and unfolds more rapidly on contact with denaturant. The amplitude of the rapid unfolding phase does not vary within this range of delay times, indicating that the slow unfolding population is formed with a rate that is extremely slow and must have a half-time of at least hours. For delay times of 1 to 30 seconds the amplitude of the slow unfolding phase was negligible or low, confirming that the native state is formed on a timescale consistent with the slowest observed refolding rate and is not formed during the observed fast phase which is complete within a few seconds under these conditions.

Slow and fast unfolding fractions coincide with the conformation of Pro166

For a number of proteins, the presence of a destabilised, fast-unfolding native-like form can be attributed to the presence of a non-native *cis-trans*

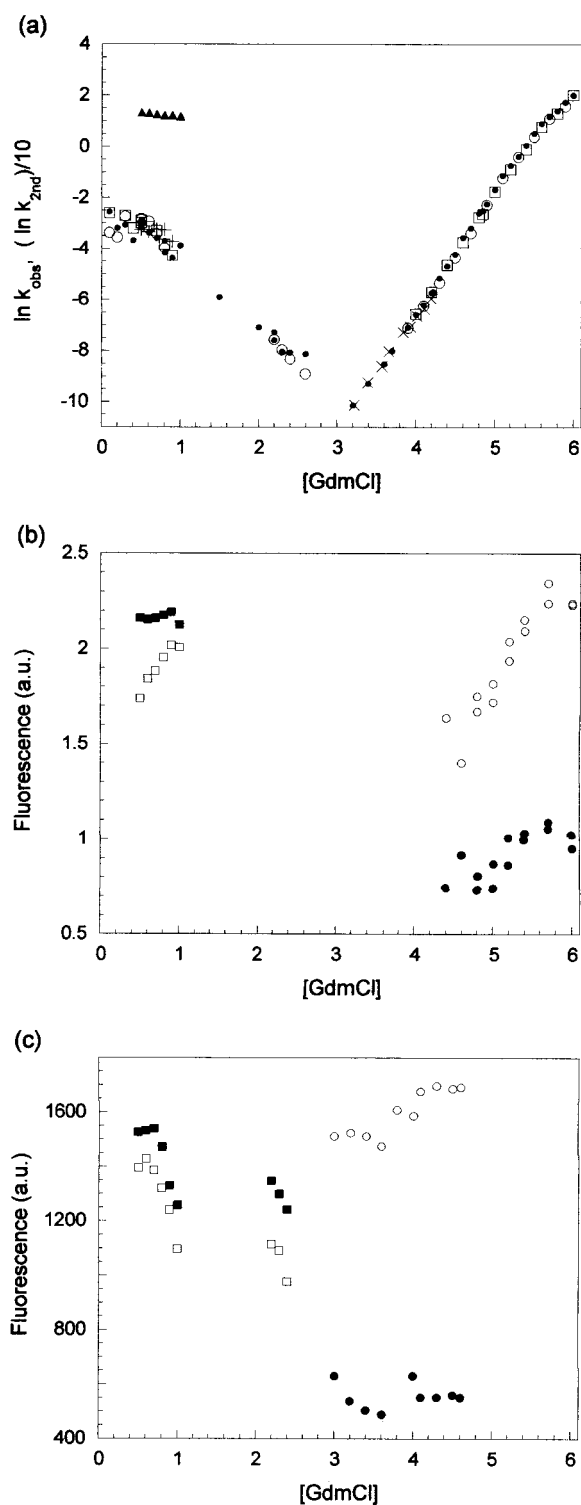


Figure 2. Denaturant dependence of the kinetic rate constants and amplitudes of unfolding and refolding of Ure2. (a) Chevron plot. Rate constants for Ure2 (\circ), 90Ure2 (\square) and $\Delta 15-42$ Ure2 (\bullet). Unfolding rate constants for protein incubated overnight in 1.5 M GdmCl (\times). Second-order rate constants for the fast phase of refolding (\blacktriangle), plotted as $(\ln k)/10$ to allow plotting on a single scale. Rate of disappearance of the dimeric intermediate measured at 1 μM protein concentration ($+$). (b) and (c) Amplitudes are expressed as initial (\square, \circ) and final (\blacksquare, \bullet) values for refolding (\square, \blacksquare) and unfolding

proline isomer.^{15,23,32,33} The observed proportion of molecules that attain the native state on the same timescale as regain of native-like fluorescence coincides with the approximately 17% of Ure2 molecules that are expected to have Pro166 in a native *cis* conformation when refolding from the fully denatured state. This would then account for the lack of further detectable refolding phases in single-jump experiments and suggests that proline isomerisation occurs after folding to a dimeric state that is spectroscopically indistinguishable from the native state.

Comparison of kinetic and equilibrium values

Refolding of Ure2 is clearly not two-state. However, within the central region of the chevron plot where the slopes are linear (Figure 2(a)), if no further kinetically significant intermediates are populated, there will be agreement between the equilibrium and kinetic values. Denaturation under equilibrium conditions yields $\Delta G_{\text{D-N,H}_2\text{O}}$, the free energy of unfolding in water. This value is the same for Ure2, 90Ure2 and $\Delta 15-42$ Ure2 (Table 1).⁷ Comparison of this value with the stability calculated from the kinetic values (obtained by linear extrapolation; Tables 1 and 2) gives a discrepancy of up to 1.7 kcal mol⁻¹ (1 kcal = 4.18 kJ; $\Delta G_{\text{D-N,H}_2\text{O}} = -RT \ln(2k_u/k_f)$; or $\Delta G_{\text{D-N,H}_2\text{O}} = -RT \ln(k_u/k_f)$, where the equilibrium transition does not involve dissociation as well as unfolding, see below). This is within the range expected due to the destabilising effect of a *cis* proline in the native state.^{23,34} The dependence of the free energy of unfolding on GdmCl concentration (*m*-value) derived from the equilibrium data (m_{eq} ; Table 1) with the equivalent value calculated from the kinetic data ($RT(m_u - m_f)$; Table 2) is the same within error.

Discussion

Ure2 has a high tendency to misfold and aggregate *in vitro*.^{6-8,10,11} A protein with biological activity defined in terms of its ability to aggregate into amyloid is an unlikely candidate for folding studies. However, if prions are truly misfolded protein forms, we cannot hope to understand this phenomenon without a thorough understanding of the folding and structural properties of the proteins that possess this activity. Significant advances in this field have

(\circ, \bullet). (b) Values measured over a short timescale (30 seconds or less) in the stopped-flow apparatus monitoring fluorescence emission using a 320 nm cut-off filter. (c) Values observed over a longer timescale (minutes to hours) measured in the fluorimeter after manual mixing and monitoring fluorescence at 327 nm.

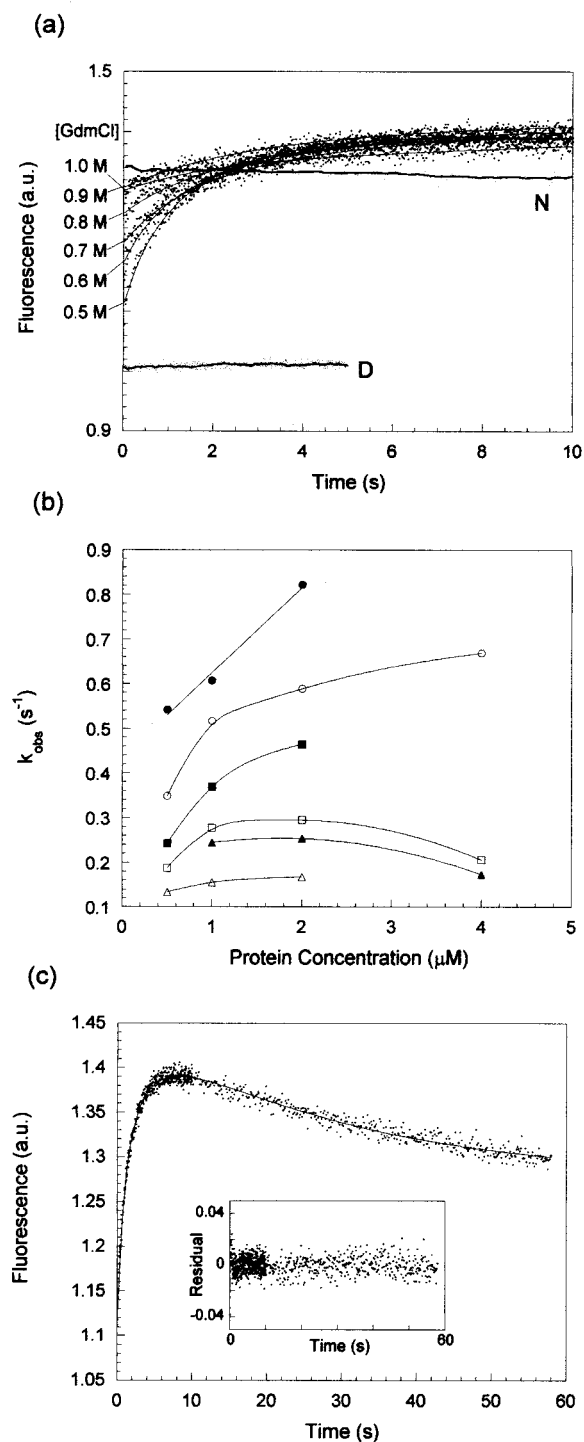


Figure 3. The burst phase and fast phase of refolding for Ure2, 90Ure2 or $\Delta 15-42$ Ure2 measured in a stopped-flow apparatus using a 320 nm cut-off filter. The protein concentration was 1 μ M unless otherwise indicated. (a) Appearance of the kinetic traces at different GdmCl concentrations (as indicated), showing the increase in the burst phase amplitude with increasing GdmCl concentration. The native state is indicated by N and denatured state as D. (b) Concentration dependence of the rate constants for the fast phase in GdmCl concentrations of 0.5 (●), 0.6 (○), 0.7 (■), 0.8 (□), 0.9 (▲) and 1.0 M (△), obtained by fitting the data to a single exponential. (c) Quality of the fit to the sum of a second-order equation and an exponential decay

been made in recent years,^{12,13,35–37} spurred on by the looming threat of a new strain of prion disease in the UK.³⁸ These advances have nevertheless been hard won due to the recalcitrant nature of these proteins and their resistance to overproduction and purification in a soluble form. It still remains unclear whether prion activity is an intrinsic property of a few rogue proteins or, if cellular co-factors are involved, how they may tip the balance between prion and normal protein forms.

Successful purification of Ure2 has been achieved in a number of laboratories.^{6–8,10} At pH 8.4, 25 °C and 1 μ M protein concentration the unfolding reaction is essentially reversible,⁷ although this reversibility is readily lost on lowering the protein concentration, temperature or pH.^{7,11} Under essentially reversible folding conditions, Ure2 shows a single equilibrium unfolding or refolding transition with mid-point 3.0 M GuHCl.⁷ The equilibrium transitions measured by fluorescence, far and near-UV CD are coincident and the spectra have isostilbic or isodichroic points.⁷ This is consistent with the occurrence of a two-state transition without the accumulation of intermediates. Equilibrium parameters reflect only the energies between states and provide no information about the pathway between them. It is common to observe two-state behaviour for the equilibrium transition even when there are stable intermediates present in water, because the population of such intermediates at denaturant concentrations around the transition region is too small to be detected.

The equilibrium folding transition shows no detectable protein concentration dependence over a 550-fold range, indicating that unfolding and dimer dissociation are not closely coupled.⁷ Chemical cross-linking studies show that dimeric structure persists after no further structural changes are detected by fluorescence or far-UV CD (L. Zhu, J. M. Zhou & S.P., unpublished results). This suggests that there is in fact a two-stage unfolding transition at pH 8.4, but the second stage, corresponding to dissociation, occurs silently within the unfolded baseline region.⁷ This is in contrast to the conclusions of Melki and co-workers, based on experiments at lower temperature and protein concentration where folding is not reversible at pH 8.4.¹¹

Under non-reversible conditions, the unfolding and refolding transitions do not coincide, due to trapping of a partially folded state (or mixture of states) during refolding.⁷ This apparent two-step

(equation (4), corresponding to formation and disappearance of a dimeric intermediate, respectively. The second-order and first-order rate constants thus obtained are plotted in Figure 2(a). The GdmCl concentration was 0.5 M.

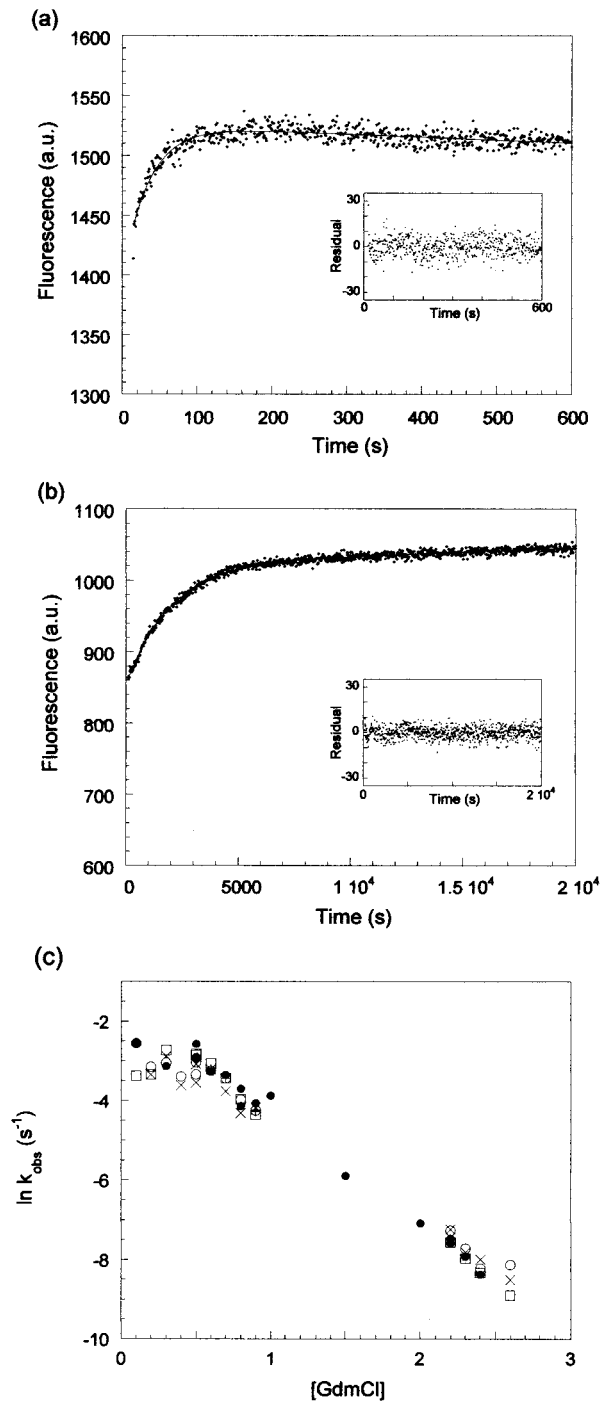


Figure 4. Slow phase of refolding for Ure2, 90Ure2 or $\Delta 15-42$ Ure2, measured in a fluorimeter by manual mixing and monitoring at 327 nm. (a) 0.5 M GdmCl, 1 μ M protein; (b) 2.2 M GdmCl, 1 μ M protein; (c) rate constants for the slow phase of refolding at 0.2 (○), 0.5 (□), 1 (●), 2 (×) and 4 (+) μ M protein concentration.

refolding transition is observed on lowering protein concentration or temperature, conditions which normally disfavour aggregation. This suggests that there is kinetic partitioning during

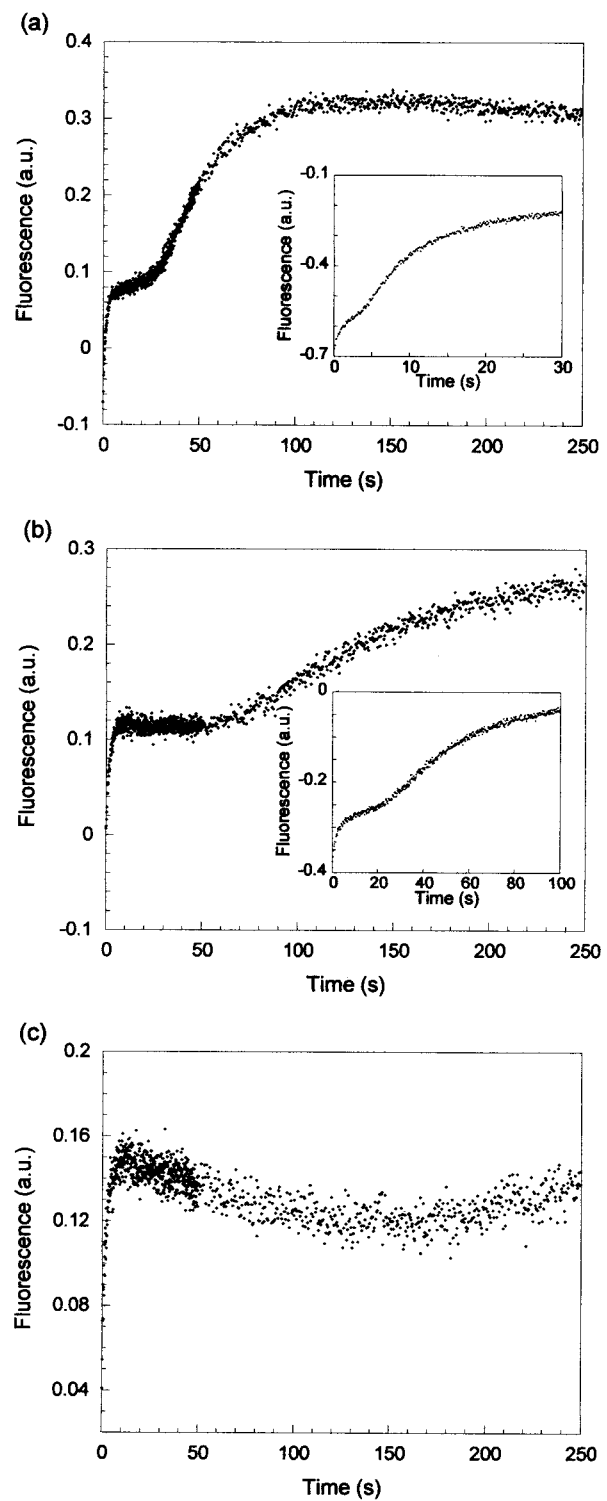


Figure 5. Observation of a lag in regain of native-like fluorescence during refolding of Ure2, 90Ure2 or $\Delta 15-42$ Ure2 measured in a stopped-flow apparatus using a 320 nm cut-off filter. The protein concentration was 2 μ M (main panels) or 4 μ M (insets). The GdmCl concentration was 0.5 M (a), 0.6 M (b) or 0.7 M (c). The lag is increased at lower protein concentration or higher GdmCl concentration, consistent with formation of an on-pathway dimeric intermediate.

folding between correct dimerisation and misfolding *via* a monomeric, aggregation prone intermediate.⁷ At lower pH, the unfolding transition like-wise shows two transitions, which is attributed to population of a stable, dimeric intermediate, although the majority of soluble protein is in the form of a high-order aggregate and folding is not reversible.¹¹

Observation of an unfolding intermediate and multiphasic unfolding kinetics

Multiphasic unfolding kinetics (Figure 1) can be due to heterogeneity in the native or denatured states, or to population of one or more intermediates during unfolding. A downturn in the unfolding arm of the chevron plot (Figure 2(a)) could be due to a switch in the rate-determining step for unfolding (e.g. from unfolding to dimer dissociation) or due to population of an unfolding intermediate. The complexity of the Ure2 unfolding kinetics indicates the involvement of more than one of these factors.

The multiphasic unfolding kinetics is not easily accounted for by heterogeneity in the native state. The presence of a non-native *cis-trans* proline isomer can give rise to a distinct native-like form.^{15,23,32,33} Ure2 has 12 proline residues, one of which (Pro166) is in a *cis* conformation in the native state.^{12,13} When Ure2 protein is fully denatured, refolded and then re-unfolded in a double-jump experiment, 80% of molecules unfold in a fast phase, corresponding to the 80% of unfolded molecules expected to have Pro166 in a non-native *trans* conformation. However, for the unfolding of never-unfolded protein this is not observed. Incubation in 1.5 M GdmCl overnight prior to unfolding has no effect on the amplitude or rate of the unfolding kinetics (Figures 1(a) and 2(a)). If distinct native-like forms are present, they must have closely similar energetic and structural properties.

In addition to “roll-over” in the unfolding rate constants (Figure 2(a)), an unfolding burst phase with a sigmoidal denaturant dependence of amplitude is also observed (Figure 2(b)). This is precisely what is predicted if there is population of an intermediate during unfolding.¹⁹ At high denaturant concentrations the native state becomes destabilised relative to this intermediate and so the intermediate becomes populated during unfolding. The population of a series of intermediates could explain the increasing complexity of the unfolding kinetics with increasing denaturant concentration. Alternatively, the additional unfolding phases may be related to heterogeneity in the denatured state.

Proline isomerisation in the denatured state subsequent to unfolding can give rise to complex unfolding kinetics, particularly for proteins containing a *cis* residue in the native state. Usually such phases are most pronounced at denaturant concentrations around the mid-point for unfolding and are no longer observed when unfolding at suf-

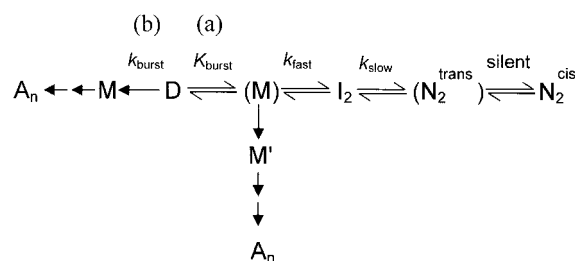
ficiently high denaturant concentration.³⁰ In contrast, for Ure2 the unfolding traces appear monophasic close to the unfolding midpoint and increase in complexity at higher GdmCl concentrations (Figure 1). One possible explanation for this is presence of residual structure in the denatured state populated in GdmCl concentrations close to the transition region. This might have the effect of simplifying the unfolding kinetics in this region. This possibility is supported by the persistence of dimeric structure in the denatured state (L. Zhu, J.M. Zhou & S.P., unpublished results). The kinetic unfolding baseline (Figure 2(b)) suggests a change in the properties of the denatured state above 5 M GdmCl. Pressure denaturation³⁹ and small angle X-ray scattering studies (L. Zhu, H. Kihara, M. Kojima, J.M. Zhou & S.P., unpublished results) of Ure2 in the presence of various concentrations of GdmCl suggest that residual structure is present in the denatured state populated in 4 to 5 M GdmCl.

The law of microscopic reversibility dictates that protein folding and unfolding reactions follow the same pathway when carried out under identical, reversible conditions. While kinetic parameters are extrapolated to the same conditions (i.e. water), in practice folding and unfolding reactions are carried out under vastly different conditions. Therefore, the intermediates detected during unfolding and refolding may be different.^{18,19,40} However, as the Ure2 unfolding intermediate has not yet been further characterised and as it is the situation in water, not high denaturant, that is relevant to the conditions encountered *in vivo*, the folding scheme proposed (Scheme 1) does not include an additional intermediate to account for the unfolding data.

An on-pathway dimeric intermediate is populated during folding

Multiple kinetic phases in refolding can arise from intermediates accumulating on a sequential pathway, or from parallel folding pathways. When an intermediate is detected, there remains the question of whether it is on or off the folding pathway (i.e. whether it offers a stepping-stone to correct folding or represents a dead-end path that must be retraced before correct folding can proceed), a topic of much interest and debate.⁴¹⁻⁴⁵ To distinguish between these possibilities is by no means straightforward even for small, monomeric proteins for which exquisite and comprehensive data are available.^{34,44}

Double-jump experiments indicate that the multiple refolding phases observed for Ure2 are not the result of parallel pathways. The presence of fast and slow phases is therefore explained by rapid formation of an intermediate followed by slow folding to the native state. The protein concentration dependence of the fast phase (Figure 3(b) and (c)) indicates that the intermediate formed is dimeric. The curvature in the denaturant depen-



Scheme 1. Minimum scheme for folding that accounts for the available data. When folding from the denatured state (D) to the native state (N_2), two intermediates are populated, an intermediate formed within the burst phase (M) and a dimeric on-pathway intermediate (I_2). The appearance of the burst phase may be due to formation of a rapid pre-equilibrium between D and M, in which case on-pathway (a) and off-pathway (not shown) schemes cannot be distinguished kinetically. Alternatively, there may be kinetic partitioning between formation of M and I_2 , where M represents an off-pathway, dead-end product (b). These and previous⁷ results suggest that M, or a subsequently formed monomeric off-pathway intermediate (M') is the precursor to the aggregation (A_n) observed during refolding of Ure2. Amyloid formation may likewise be a multi-step process stemming from a common precursor (i.e. D or M). Isomerisation of Pro166 to the native *cis* form is not limiting for folding, but occurs subsequent to regain of native-like fluorescence.

dence of the slow refolding rate constants at low denaturant concentrations is consistent with the population of the dimeric intermediate under these conditions (Figure 2(a)). Whether an intermediate is on or off-pathway can theoretically be distinguished from the kinetics. The definitive test for an on-pathway intermediate is the observation of a lag in formation of the native state. In practice there are limited examples where this has been possible^{31,40,46–50} and detection has usually required that folding is fortuitously slow and/or the means to detect individual species within the complex folding mixture.

The strong change in the Ure2 fluorescence emission spectrum on unfolding⁷ makes fluorescence spectroscopy a sensitive technique for monitoring the folding reaction. The main disadvantage of the method is that the observed fluorescence signal represents the sum of signals for all species present in solution. The lack of an assay for enzymatic activity precludes the use of this method to monitor regain of native Ure2, distinct from the other species present. However, we found that a lag in formation of native Ure2, subsequent to formation of the dimeric intermediate, could nevertheless be detected by fluorescence (Figure 5), aided by the fact that detection could be biased towards observation of the native state or partially folded species by varying the emission wavelength(s) monitored. This property may be useful in further investi-

gations of the intermediate states populated during folding. The lag in appearance of the native-like state was longer at lower protein concentration or higher GdmCl concentration (Figure 5), consistent with the formation of an on-pathway dimeric intermediate. Where the lag was long, disappearance of the dimeric intermediate could be detected prior to appearance of the native-like state (Figures 3(c) and 5(c)). The rate of disappearance of the dimeric intermediate was equal to the rate of appearance of native-like fluorescence (Figure 2(a)), consistent with a lack of further populated intermediates on the folding pathway. This is also suggested by the agreement between equilibrium and kinetic *m*-values in this region (Tables 1 and 2; see also Results).

Observation of a burst phase refolding intermediate

Where an intermediate is formed rapidly within the dead-time of mixing, on and off-pathway folding schemes cannot usually be distinguished because they are kinetically equivalent.^{34,44} The observation of a burst phase in Ure2 refolding could suggest that a rapid pre-equilibrium is established between the fully denatured state and the burst phase intermediate (Scheme 1(a)). The increase in amplitude with increasing denaturant concentration (Figure 3(a)) would then suggest that the stability of this burst phase intermediate relative to the more fully denatured state increases with GdmCl concentration within this range (0.5 to 1.0 M). In general, the less compact state is expected to be favoured at increased denaturant concentration. However, it must be born in mind that GdmCl is not only a denaturant, but also a salt, which could have a stabilising effect on compact states.

Alternatively, kinetic partitioning between the on-pathway dimeric intermediate and this burst phase intermediate could explain the relative changes in the amplitudes of the two phases (Figure 3(a)). In this case, the burst phase intermediate would necessarily be off-pathway (or at least on a parallel pathway). As the observed kinetics suggests a single, sequential folding pathway, this would then suggest that the burst phase intermediate is a dead-end product (Scheme 1(b)).

Role of intermediates in aggregation and amyloid formation

Where the dimeric intermediate is significantly populated during refolding, aggregation is negligible. As population of the dimeric intermediate decreases and population of the burst phase intermediate increases, the final fluorescence yield falls (Figure 2), indicating the increased occurrence of a non-productive side-reaction. The protein concentration and temperature dependence of hysteresis in the refolding curves measured under equilibrium conditions strongly suggests that there is

kinetic partitioning between correct folding *via* dimerisation and misfolding *via* a monomeric intermediate.⁷ This suggests that the burst phase intermediate may be this misfolded, aggregation prone intermediate or may be a precursor to its formation (Scheme 1). This also suggests that correct dimerisation protects the protein from non-productive side-reactions during folding.

The key characteristic of mechanisms proposed to account for seeded formation of amyloid is the presence of assembly competent (i.e. misfolded or aggregation-prone) and assembly non-competent (i.e. correctly folded) forms.^{51–54} The observation of two different folding intermediates, as presented here, provides a structural basis for such a mechanism in the case of Ure2. A recent study suggests that for amyloid formation of the yeast prion Sup35, the precursor first forms an assembly-competent oligomer, which can then interact efficiently with the growing fibril.⁵³ Ure2 amyloid formation may likewise be a multi-step process.

Incubation of native Ure2 *in vitro* tends to produce amorphous aggregates rather than amyloid.^{6,10} Amyloid formation can be induced by addition of PrD as a synthetic peptide or by addition of a preformed seed,⁶ which reduces the lag time in fibre formation.^{8,10} In some cases, addition of preformed fibrils was observed to seed both amyloid and aggregate formation.¹⁰ Amyloid formation is favoured at lower pH where the dimeric intermediate is apparently stabilised, but aggregation is increased.¹¹ This indicates that for Ure2, aggregation and amyloid formation represent competing reactions, possibly stemming from a common precursor (Scheme 1). Amyloid formation will be favoured both by optimum population of the amyloid precursor and by minimisation of competing side-reactions that form amorphous aggregates.

Even under conditions where intermediates are unstable and only transiently populated, they can be trapped and stabilised by formation of a high-order oligomer, as in aggregation or amyloid formation. Where oligomerisation is irreversible (or only slowly reversible), the presence of a dynamic equilibrium between native, denatured and intermediate states means that potentially the entire population of molecules can be drawn off to the misfolded, oligomeric state *via* one or more assembly-competent intermediates, whether the intermediate is on or off-pathway (Scheme 1).

The favouring of amyloid formation at pH 7.5 compared to pH 8.4¹¹ and the observed formation of Ure2 PrD fibres in bacterial extracts¹⁰ may explain an earlier puzzling finding,⁷ namely that Ure2 could be solubilised from *Escherichia coli* cells at pH 8.4 but not pH 7.5, whereas both values of pH could be used for constructs lacking the prion domain. $\Delta 15-42$ Ure2 fell into the category of variants that could be purified at pH 7.5 and is found empirically to be the most soluble of the Ure2 variants we have constructed.⁷ This suggests a direct

role for residues 15-42 of Ure2 in amyloid formation.

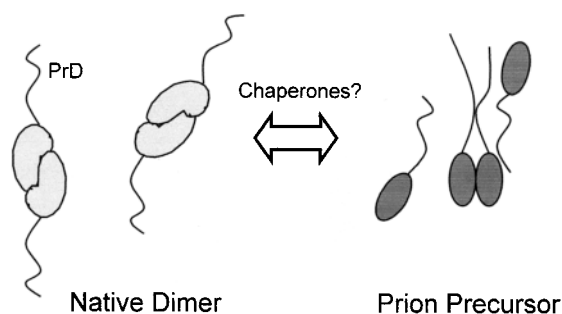
Role of the PrD in prion formation

The N-terminal PrD is necessary and sufficient for induction and propagation of the prion form of Ure2 *in vivo*^{9,55} and amyloid formation *in vitro*.^{6,10} The PrD is highly susceptible to proteolysis, suggesting that it is unstructured in the native state.^{7,8,13} Equilibrium denaturation experiments show that deletion of all or parts of the PrD has no effect on the thermodynamic stability or the degree of exposure to solvent (*m*-value) on unfolding, which strongly implies that the PrD is unstructured and does not interact with the C-terminal region in the native state.⁷ The results presented here and a qualitative comparison of the effect of the PrD on the characteristics of the denaturation curves over a wide range of conditions of pH¹¹ also indicate that the PrD does not affect the stability or folding of Ure2, suggesting that N and C-terminal regions do not interact.

In apparent contradiction to this, *in vivo* studies indicate that the C-terminal nitrogen regulatory region stabilises the protein against prion formation.^{9,56} A number of seven to eight residue deletions in the C-terminal region have been shown to enhance or prevent prion induction.^{9,57} Pairs of point mutations in the PrD and C-terminal region suggest that the two regions function synergistically to induce prion formation.⁵⁶ This implies that direct interaction between the C-terminal region and the PrD plays an important role in regulating prion induction.

This apparent contradiction is explained if prion formation requires unhindered association of prion domains, which is sterically blocked in the native dimeric structure,⁷ but is possible in a partially folded precursor (Scheme 2). This model is supported by a number of findings: native Ure2 does not readily form amyloid, but amyloid formation is efficiently induced by addition of PrD as a synthetic peptide;⁶ insertion of a spacer between the PrD and a heterologous fusion protein increases the efficiency of PrD-dependent amyloid formation,¹⁰ and inspection of the crystal structure shows that the N termini are diametrically opposed in the folded dimer.^{12,13} Interaction between N and C-terminal regions may be important at the stage of assembly of the prion precursor into amyloid or into an assembly-competent oligomer, steps that are out of the range of detection of the folding studies presented here and previously.⁷

The above hypothesis allows for a number of mechanisms by which mutations or deletions in the C-terminal region could affect prion induction. Prion formation could be favoured or disfavoured by altering the stability of the prion precursor, or by altering the relative stability of the native or other intermediate states. Mutations could also alter the self-association properties of the prion precursor. A tendency to self-associate may play



Scheme 2. A putative model for Ure2 prion formation which accounts for the apparent contradiction between *in vivo* and *in vitro* results. In the native dimer the N-terminal prion domain (PrD) is unstructured and interaction with the C-terminal region is sterically disfavoured. In the prion precursor, prion domains are able to align in a manner which allows amyloid formation. The unstructured nature of the PrD may be important for interaction with chaperones, which may assist in the structural transition to form the prion precursor. Mutations that affect prion formation may act by changing the stability or self-association properties of the prion precursor, or by affecting the relative population of other states.

an important role in amyloid formation by bringing prion domains into close proximity and thus increasing the effective concentration. A role of both the PrD and the C-terminal region in this assembly process would account for the observation of compensatory mutations in the N and C-terminal regions.^{56,57}

A further possibility is that some or all of the mutations or deletions identified^{9,56,57} affect interaction with cellular cofactors.¹³ A recent study indicates the involvement of molecular chaperones in Ure2 prion propagation *in vivo*.⁵⁸ The chaperones may bind to and stabilise the prion precursor and/or may facilitate the unfolding reaction that allows population of this precursor. The unstructured nature of the prion domain in the native state may be important in prion formation by facilitating interaction with chaperones or other cellular cofactors.

Materials and Methods

Materials

Chemicals and reagents were obtained from BDH, Pierce or Sigma. Solutions were made volumetrically.

Protein production and purification

Ure2 and N-terminal variants, 90Ure2 and Δ 15-42Ure2, were produced in *E. coli* and purified as described.⁷ 90Ure2 lacks the glutamine/asparagine-rich region from residues 1-89 and therefore lacks the entire PrD as defined either by biological activity⁵⁷ or inspection of the protein sequence.⁷ Δ 15-42Ure2 contains the

entire glutamine/asparagine-rich region but the small region of "normal" amino acid sequence from residue 15 to 42 has been excised.⁷ All proteins were produced with a short N-terminal histidine tag to allow a high level of purity to be achieved. The tag was left intact for further studies and not proteolytically cleaved because of the susceptibility of Ure2 to proteolysis.^{7,8,13} His-tagged Ure2 has normal biological activity *in vivo*,⁵⁹ amyloid forming ability *in vitro*⁶ and the same oligomeric structure, stability and equilibrium folding behaviour as untagged protein.⁷

Stopped-flow kinetics

The kinetics of Ure2 and N-terminal variants 90Ure2 and Δ 15-42Ure2 refolding and unfolding were monitored using an Applied Photophysics (Surrey, UK) SX17 stopped-flow apparatus, or in an Aminco Bowman series 2 luminescence spectrometer after manual mixing for measurement of slower rates or for dilutions of greater than 1:10. Excitation was at 280 nm. Emission was monitored in the stopped-flow apparatus at 327 nm using a monochromator or above 320 nm using a cut-off filter. Monitoring in the Aminco Bowman machine was at 327 nm. Native protein has a maximum emission wavelength of 334 nm, whereas the maximum change in fluorescence signal on unfolding occurs at 327 nm.⁷ It was found that monitoring with a 320 nm cut-off filter biases detection towards monitoring of partially folded species and emphasises the lag in appearance of the native state, whereas detection at a single wavelength of 327 nm biases towards detection of the native (or native-like) state. The experimental set-up therefore affects the relative fluorescence changes observed. Hence at 1 μ M protein concentration where the lag is long, maximal population of the dimeric intermediate results in a fluorescence yield using a cut-off filter slightly higher than that of the native state and disappearance of this intermediate during the lag is apparent. When monitoring at a single wavelength, disappearance of the intermediate is not apparent and the regain of fluorescence during the fast phase is slightly lower than that of the native state. The exponential fall in fluorescence intensity observed using a cut-off filter is not affected by varying the slit widths and the same decrease is observed when measuring endpoints after a delay with the shutter closed. Therefore this decrease in fluorescence is not due to photolysis.

Rates measured under the same conditions in the two instruments were the same. All experiments were performed in 50 mM Tris-HCl (pH 8.4), with 200 mM NaCl. The final protein concentration was 1 μ M and the temperature 25 °C unless otherwise stated. For unfolding, protein in buffer was diluted into buffer containing a range of GdmCl concentrations to give a final GdmCl concentration of greater than 3.1 M. For refolding, protein was first denatured in 4.5 M or higher concentration GdmCl in buffer and incubated for sufficient time to ensure complete unfolding. (Typically 5.5 M GdmCl was used, where unfolding is complete within seconds.) The denatured protein was then diluted with buffer containing no or low concentration of GdmCl to give a final GdmCl concentration of less than 3.0 M. Data were fitted to equations indicated using the program Kaleidagraph (Synergy Software).

Double-jump stopped-flow experiments

To perform double-jump refolding under conditions limited for proline isomerisation, the protein was unfolded for five seconds in 5.4 M GdmCl where the half-life of unfolding is one second. Isomerisation of proline residues during this delay time is expected to be negligible.²³ Refolding was then initiated by 1:10 mixing with buffer (with or without low concentrations of GdmCl) to give a final GdmCl concentration of 0.49 M or greater. Under these conditions it is assumed that the majority of protein molecules refold with all proline residues in a native conformation. These experiments were performed in the sequential mode of the stopped-flow apparatus. Double-jump unfolding experiments were performed in an analogous manner by first denaturing protein in 5.5 M GdmCl. Refolding was initiated by mixing 1:10 with buffer and was allowed to proceed for various delay times (one second to one hour). The protein was then re-unfolded by mixing 1:1 with 8 M GdmCl. For delay times of one minute to one hour the experiments were performed by manual mixing.

Aggregation observed during refolding

Ure2 could not be unfolded by acid or alkali and has a high tendency to aggregate even at micromolar concentrations, both of which place limits on the reaction conditions that are accessible to experiment. The acquisition of refolding data was further complicated by the tendency of the protein to aggregate when refolding in moderate concentrations of GdmCl (1.0 to 2.0 M) under all conditions of protein concentration (0.2 to 5 μ M) and temperature (10 to 30 °C) sampled. No aggregation was visible to the eye, but light scattering (not shown) and velocity sedimentation (S.P. & P.J.G. Butler, unpublished results) confirms the presence of soluble aggregates under these conditions, which clearly reduces the quality of the kinetic data that could be acquired. Steady-state experiments suggest that the aggregation is at least partially reversible.²⁴ No aggregation was detected by light scattering within a 24 hour period when refolding in 0.6 M GdmCl under these conditions (not shown).

Acknowledgements

We thank Professor J.M. Zhou, Dr Laura Itzhaki, Dr Chris Johnson, Dr Teikichi Ikura and Ugo Mayor for helpful discussions and expert advice. We thank L. Zhu for repeating some of the refolding experiments. This work was supported in part by a grant from the BBSRC. S.P. acknowledges support from the Royal Society, the Royal Commission for the Exhibition of 1851 and Sidney Sussex College, Cambridge.

References

- Prusiner, S. B. (1998). Prions. *Proc. Natl Acad. Sci. USA*, **95**, 13363-13383.
- Wickner, R. B., Taylor, K. L., Edskes, H. K., Maddelein, M. L., Moriyama, H. & Roberts, B. T. (2000). Prions of yeast as heritable amyloidoses. *J. Struct. Biol.* **130**, 310-322.
- Lindquist, S. (1997). Mad cows meet psi-chotic yeast: the expansion of the prion hypothesis. *Cell*, **89**, 495-498.
- Lacroute, F. (1971). Non-Mendelian mutation allowing ureidosuccinic acid uptake in yeast. *J. Bacteriol.* **106**, 519-522.
- Wickner, R. B. (1994). [URE3] as an altered URE2 protein: evidence for a prion analog in *Saccharomyces cerevisiae*. *Science*, **264**, 566-569.
- Taylor, K. L., Cheng, N., Williams, R. W., Steven, A. C. & Wickner, R. B. (1999). Prion domain initiation of amyloid formation *in vitro* from native Ure2p. *Science*, **283**, 1339-1342.
- Perrett, S., Freeman, S. J., Butler, P. J. G. & Fersht, A. R. (1999). Equilibrium folding properties of the yeast prion protein determinant Ure2. *J. Mol. Biol.* **290**, 331-345.
- Thual, C., Komar, A. A., Bousset, L., Fernandez-Bellot, E., Cullin, C. & Melki, R. (1999). Structural characterization of *Saccharomyces cerevisiae* prion-like protein Ure2. *J. Biol. Chem.* **274**, 13666-13614.
- Masison, D. C. & Wickner, R. B. (1995). Prion-inducing domain of yeast Ure2p and protease resistance of Ure2p in prion-containing cells. *Science*, **270**, 93-95.
- Schlumpberger, M., Wille, H., Baldwin, M. A., Butler, D. A., Herskowitz, I. & Prusiner, S. B. (2000). The prion domain of yeast Ure2p induces autocatalytic formation of amyloid fibers by a recombinant fusion protein. *Protein Sci.* **9**, 440-451.
- Thual, C., Bousset, L., Komar, A., Walter, S., Buchner, J., Cullin, C. & Melki, R. (2001). Stability, folding, dimerization, and assembly properties of the yeast prion Ure2p. *Biochemistry*, **40**, 1764-1773.
- Bousset, L., Belrhali, H., Janin, J., Melki, R. & Morera, S. (2001). Structure of the globular region of the prion protein Ure2 from the yeast *Saccharomyces cerevisiae*. *Structure*, **9**, 39-46.
- Umlaud, T. C., Taylor, K. L., Rhee, S., Wickner, R. B. & Davies, D. R. (2001). The crystal structure of the nitrogen regulation fragment of the yeast prion protein Ure2p. *Proc. Natl Acad. Sci. USA*, **98**, 1459-1464.
- Coshigano, P. W. & Magasanik, B. (1991). The URE2 gene product of *Saccharomyces cerevisiae* plays an important role in the cellular response to the nitrogen source and has homology to glutathione S-transferases. *Mol. Cell. Biol.* **11**, 822-832.
- Rousseau, F., Schymkowitz, J. W. H., Sanchez del Pino, M. & Itzhaki, L. S. (1998). Stability and folding of the cell cycle regulatory protein, p13(suc1). *J. Mol. Biol.* **284**, 503-519.
- Matouschek, A. & Fersht, A. R. (1993). Application of physical organic chemistry to engineered mutants of proteins: Hammond postulate behavior in the transition state of protein folding. *Proc. Natl Acad. Sci. USA*, **90**, 7814-7818.
- Matouschek, A., Otzen, D. E., Itzhaki, L. S., Jackson, S. E. & Fersht, A. R. (1995). Movement of the position of the transition state in protein folding. *Biochemistry*, **34**, 13656-13662.
- Jonsson, T., Waldburger, C. D. & Sauer, R. T. (1996). Non-linear free energy relationships in Arc repressor unfolding imply the existence of unstable, native-like folding intermediates. *Biochemistry*, **35**, 4795-802.
- Zaidi, F. N., Nath, U. & Udgaonkar, J. B. (1997). Multiple intermediates and transition states during protein unfolding. *Nature Struct. Biol.* **4**, 1016-1024.
- Mateu, M. G., Sanchez Del Pino, M. M. & Fersht, A. R. (1999). Mechanism of folding and assembly of a small tetrameric protein domain from tumor suppressor p53. *Nature Struct. Biol.* **6**, 191-198.

21. Silow, M. & Oliveberg, M. (1997). Transient aggregates in protein folding are easily mistaken for folding intermediates. *Proc. Natl Acad. Sci. USA*, **94**, 6084-6086.
22. Matouschek, A., Kellis, J. T., Serrano, L., Bycroft, M. & Fersht, A. R. (1990). Transient folding intermediates characterized by protein engineering. *Nature*, **346**, 440-445.
23. Schreiber, G. & Fersht, A. R. (1993). The refolding of *cis*- and *trans*-peptidylprolyl isomers of barstar. *Biochemistry*, **32**, 11195-11203.
24. Capaldi, A. P., Ferguson, S. J. & Radford, S. E. (1999). The Greek key protein apo-pseudoazurin folds through an obligate on-pathway intermediate. *J. Mol. Biol.* **286**, 1621-1632.
25. Jackson, S. E. & Fersht, A. R. (1991). Folding of chymotrypsin inhibitor 2. 2. Influence of proline isomerization on the folding kinetics and thermodynamic characterization of the transition state of folding. *Biochemistry*, **30**, 10436-10443.
26. Kiefhaber, T. & Schmid, F. X. (1992). Kinetic coupling between protein folding and prolyl isomerization. I. Folding of ribonuclease A and ribonuclease T₁. *J. Mol. Biol.* **224**, 231-240.
27. Schmid, F. X. & Blaschek, H. (1981). A native-like intermediate on the ribonuclease A pathway. 2. Comparison of its properties to native ribonuclease. *Eur. J. Biochem.* **114**, 111-117.
28. Evans, P. A., Kautz, R. A., Fox, R. O. & Dobson, C. M. (1989). A magnetization-transfer nuclear magnetic resonance study of the folding of staphylococcal nuclease. *Biochemistry*, **28**, 363-370.
29. Nakano, T., Antonio, L. C., Fox, R. O. & Fink, A. L. (1993). Effect of proline mutations on the stability and kinetics of folding of staphylococcal nuclease. *Biochemistry*, **32**, 2534-2541.
30. Brandts, J. F., Halvorson, H. R. & Brennan, M. (1975). Consideration of the possibility that the slow step in protein denaturation reactions is due to *cis*-*trans* isomerisation of proline residues. *Biochemistry*, **14**, 4953-4963.
31. Schmid, F. X. (1983). Mechanism of folding of ribonuclease A. Slow refolding is a sequential reaction *via* intermediates. *Biochemistry*, **22**, 4690-4696.
32. Sugawara, T., Kuwajima, K. & Sugai, S. (1991). Folding of staphylococcal nuclease A studied by equilibrium and kinetic circular dichroism spectra. *Biochemistry*, **30**, 2698-2706.
33. Zitzewitz, J. A. & Matthews, C. R. (1999). Molecular dissection of the folding mechanism of the alpha subunit of tryptophan synthase: an amino-terminal autonomous folding unit controls several rate-limiting steps in the folding of a single domain protein. *Biochemistry*, **38**, 10205-10214.
34. Fersht, A. R. (1999). *Structure and Mechanism in Protein Science*, Freeman, San Francisco.
35. Riek, R., Hornemann, S., Wider, G., Billeter, M., Glockshuber, R. & Wuthrich, K. (1996). NMR structure of the mouse prion protein domain PrP(121-321). *Nature*, **382**, 180-182.
36. Jackson, G. S., Hosszu, L. L. P., Power, A., Hill, A. F., Kenney, J., Saibil, H. *et al.* (1999). Reversible conversion of monomeric human prion protein between native and fibrillogenic conformations. *Science*, **283**, 1935-1937.
37. Zahn, R., Liu, A., Luhrs, T., Riek, R., von Schroetter, C., Lopez Garcia, F. *et al.* (2000). NMR solution structure of the human prion protein. *Proc. Natl Acad. Sci. USA*, **97**, 145-150.
38. Collinge, J. (1999). Variant Creutzfeldt-Jakob disease. *Lancet*, **354**, 317-323.
39. Zhou, J. M., Zhu, L., Balny, C. & Perrett, S. (2001). Pressure denaturation of the yeast prion protein Ure2. *Biochem. Biophys. Res. Commun.* **287**, 147-152.
40. Walkenhorst, W. F., Green, S. M. & Roder, H. (1997). Kinetic evidence for folding and unfolding intermediates in staphylococcal nuclease. *Biochemistry*, **36**, 5795-5805.
41. Creighton, T. E. (1994). The energetic ups and downs of protein-folding. *Nature Struct. Biol.* **1**, 135-138.
42. Fersht, A. R. (1995). Optimization of rates of protein-folding - the nucleation-condensation mechanism and its implications. *Proc. Natl Acad. Sci. USA*, **92**, 10869-10873.
43. Baldwin, R. L. (1996). On-pathway versus off-pathway folding intermediates. *Fold. Des.* **1**, R1-R8.
44. Roder, H. & Colon, W. (1997). Kinetic role of early intermediates in protein folding. *Curr. Opin. Struct. Biol.* **7**, 15-28.
45. Fersht, A. R. (2000). A kinetically significant intermediate in the folding of barnase. *Proc. Natl Acad. Sci. USA*, **97**, 14121-14126.
46. Ziegler, M. M., Goldberg, M. E., Chaffotte, A. F. & Baldwin, T. O. (1993). Refolding of luciferase subunits from urea and assembly of the active heterodimer. *J. Biol. Chem.* **268**, 10760-10765.
47. Heidary, D. K., Gross, L. A., Roy, M. & Jennings, P. A. (1997). Evidence for an obligatory intermediate in the folding of interleukin-1 β . *Nature Struct. Biol.* **4**, 725-731.
48. Farooq, A. (1998). Kinetic evidence for an obligatory intermediate in the folding of the membrane protein bacteriorhodopsin. *Biochemistry*, **37**, 15170-15176.
49. Szilagyi, A. N. & Vas, M. (1998). Sequential domain refolding of pig muscle 3-phosphoglycerate kinase: kinetic analysis of reactivation. *Fold. Des.* **3**, 565-575.
50. Heidary, D. K., O'Neill, J. C., Roy, M. & Jennings, P. A. (2000). An essential intermediate in the folding of dihydrofolate reductase. *Proc. Natl Acad. Sci. USA*, **97**, 5866-5870.
51. Griffith, J. S. (1967). Self-replication and scrapie. *Nature*, **215**, 1043-1044.
52. Jarrett, J. T. & Lansbury, P. T., Jr (1993). Seeding "one dimensional crystallization" of amyloid: a pathogenic mechanism in Alzheimer's disease and scrapie?. *Cell*, **73**, 1055-1058.
53. Serio, T. R., Cashikar, A. G., Kowal, A. S., Sawicki, G. J., Moslehi, J. J., Serpell, L. *et al.* (2000). Nucleated conformational conversion and the replication of conformational information by a prion determinant. *Science*, **289**, 1317-1321.
54. Kelly, J. W. (2000). Mechanisms of amyloidogenesis. *Nature Struct. Biol.* **7**, 824-826.
55. Masison, D. C., Maddelein, M. L. & Wickner, R. B. (1997). The prion model for [URE3] of yeast: spontaneous generation and requirements for propagation. *Proc. Natl Acad. Sci. USA*, **94**, 12503-12508.
56. Fernandez-Bellot, E., Guillement, E. & Cullin, C. (2000). The yeast prion [URE3] can be greatly induced by a functional mutated URE2 allele. *EMBO J.* **19**, 3215-3222.
57. Maddelein, M. L. & Wickner, R. B. (1999). Two prion-inducing regions of Ure2p are nonoverlapping. *Mol. Cell. Biol.* **19**, 4516-4524.

58. Moriyama, H., Edskes, H. K. & Wickner, R. B. (2000). [URE3] Prion propagation in *Saccharomyces cerevisiae*: requirement for chaperone Hsp104 and curing by overexpressed chaperone Ydj1p. *Mol. Cell. Biol.* **20**, 8916-8922.
59. Komar, A. A., Guillement, E., Reiss, C. & Cullin, C. (1998). Enhanced expression of the yeast Ure2 protein in *Escherichia coli*: the effect of synonymous codon substitutions at a selected place in the gene. *Biol. Chem.* **379**, 1295-1300.

Edited by J. Karn

(Received 30 July 2001; received in revised form 5 November 2001; accepted 8 November 2001)